

Angle-of-Attack Control of Drag for Slender Re-entry Vehicle Recovery

D.H. Platus*

The Aerospace Corporation, El Segundo, Calif.

A method is described in which drag increase due to angle of attack is used to decelerate a slender, high-ballistic-coefficient re-entry vehicle for recovery. The angle of attack and drag increase are produced by the application of a controlled wind-fixed yaw moment which causes dynamic undamping of the angle of attack. A small yaw moment can induce large circular coning motion for which the drag is predictable. It is shown that sufficient deceleration for recovery can be obtained after the vehicle has experienced high stagnation pressures for nosetip and heat-shield testing. Practical implementation of the recovery system is discussed.

Nomenclature

A_N	= normal acceleration, g's
C_D	= aerodynamic drag coefficient
C_L	= aerodynamic lift coefficient
$C_{m_q} + C_{m_{\dot{\alpha}}}$	= aerodynamic pitch damping derivative
C_N	= aerodynamic normal force coefficient
C_N^α	= aerodynamic normal force derivative
C_{Y_β}	= aerodynamic side force derivative
d	= base diameter (reference length)
F_y	= applied yaw force
g	= acceleration due to gravity
h	= altitude
I	= pitch or yaw moment of inertia
I_x	= roll moment of inertia
L	= vehicle length
m	= vehicle mass
M_y	= applied yaw moment
p	= roll rate
Q	= dynamic pressure
R_E	= Earth radius
S	= aerodynamic reference area (base area)
t	= time
u	= vehicle velocity
u_E	= entry velocity
x_c	= yaw force moment arm
x_{st}	= static margin (distance of center of pressure aft of center of gravity)
γ	= path angle
γ_E	= entry path angle
ζ	= aerodynamic pitch or yaw damping ratio
θ	= angle of attack (coning half-angle)
θ_0^*	= nonrolling trim angle of attack due to a body-fixed moment of magnitude M_y
μ	= I_x / I
ρ	= atmospheric density
$\dot{\phi}$	= windward-meridian rotation rate
$\dot{\phi}_+$	= characteristic windward-meridian rotation frequencies
$\dot{\psi}_+$	= characteristic precession frequencies
ω	= natural pitch frequency

I. Introduction

IT was shown recently¹ that the angle of attack (coning angle) of a spinning or nonspinning missile can be controlled by the application of a controlled wind-fixed yaw moment. Very small yaw moments are required in order to produce large angles of attack, and the resulting circular coning motion is found to be stable and well-behaved. The application of yaw-moment undamping of angle of attack to increase the drag for recovery of a re-entry vehicle is investigated in the present paper. This concept of recovery has several advantages over other recovery concepts that require a drastic configuration change to produce sufficient drag. With angle-of-attack control, the entire vehicle is recovered, which permits maximum on-board experimentation and instrumentation. The concept has no size limitations and applies to both large and small vehicles. The recovery system size and weight are minimal because of the small yaw moment required to undamp the angle of attack. The drag increase with angle of attack is so great that recovery can be initiated at altitudes as low as 10 to 15 kft, after the vehicle has been subjected to high stagnation pressures for nosetip and heat-shield testing. Yaw moment undamping of angle of attack produces a rapidly rotating wind-ward meridian which distributes the heat load uniformly around the heat shield. The recovery energy is therefore dissipated in heating over the entire vehicle.

The recovery concept is investigated for a 9 deg half-angle, sharp conical vehicle with a hypersonic ballistic coefficient of approximately 2500 psf. A zero angle-of-attack reference trajectory is selected that gives a peak dynamic pressure of approximately 130,000 psf at 24 kft. Recovery is initiated at several altitudes below 24 kft, and the angle of attack required for recovery is calculated from integration of the trajectory equations, with the constraint that the lateral acceleration due to angle of attack is held constant. The control moment required to generate the angle of attack is calculated from the steady-state theory derived earlier¹ and is compared with computer simulations of the coupled rotational and trajectory equations of motion. Implementation of the recovery system is discussed.

II. Angle-of-Attack Requirements

The trajectory equations can be written

$$\dot{u} = -\frac{C_D(\theta)\rho u^2 S}{2m} + g \sin \gamma \quad (1)$$

$$\dot{h} = -u \sin \gamma \quad (2)$$

$$\dot{\gamma} = \left(\frac{g}{u} - \frac{u}{R_E + h} \right) \cos \gamma \quad (3)$$

Received Oct. 7, 1975; presented as Paper 75-1357 at The AIAA 5th Aerodynamic Deceleration Systems Conference, Albuquerque, N. Mex., Nov. 17-19, 1975; revision received Feb. 6, 1976. This work was supported by the U.S. Air Force under Contract No. F04701-75-C-0076. The author is grateful to M.E. Brennan for her able assistance with the numerical computations.

Index categories: LV/M Dynamics and Control; LV/M Aerodynamics.

*Senior Staff Scientist, Aerophysics Laboratory. Member AIAA.

where $C_D(\theta)$ is the drag coefficient as a function of the coning half-angle or angle of attack θ . These equations are integrated subject to the constraint on angle of attack that the normal acceleration A_N , defined by

$$A_N = \frac{\rho u^2 S}{2mg} [C_L(\theta) \cos \theta + C_D(\theta) \sin \theta] \quad (4)$$

remains constant. This condition is imposed with the assumption that the normal load factor could be structurally limiting.

Experimental lift and drag data for a sharp 9 deg cone at several hypersonic Mach numbers are shown in Fig. 1.² The data at Mach 6.77, covering the full angle-of-attack range, were used in the simulations as representative of average conditions during recovery. The drag increase as a ratio of the drag coefficient at angle of attack to the zero angle-of-attack value is shown in Fig. 2. A zero angle-of-attack reference trajectory is shown in Fig. 3, calculated for a ratio of vehicle mass to reference area m/S of 5.5 slug/ft², which corresponds to a hypersonic ballistic coefficient of approximately 2500 psf.

Results of numerical integrations for recovery velocity and required angle of attack are shown in Fig. 4 for different altitudes of recovery initiation. The angle of attack was calculated to decelerate the vehicle to Mach 1 by 2 kft at constant normal acceleration. Maximum angles of attack were

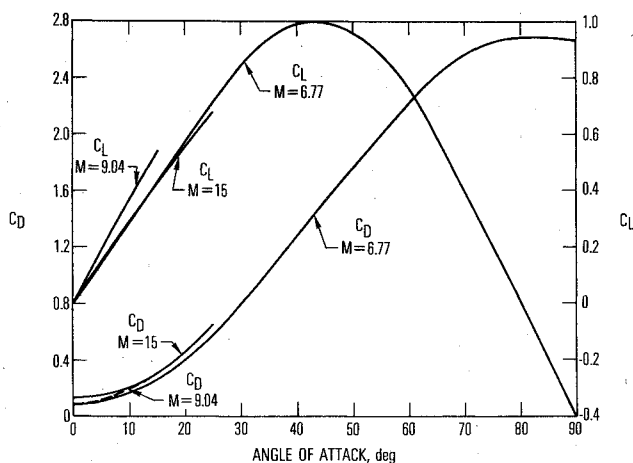


Fig. 1 Hypersonic aerodynamics of sharp 9 deg cone.

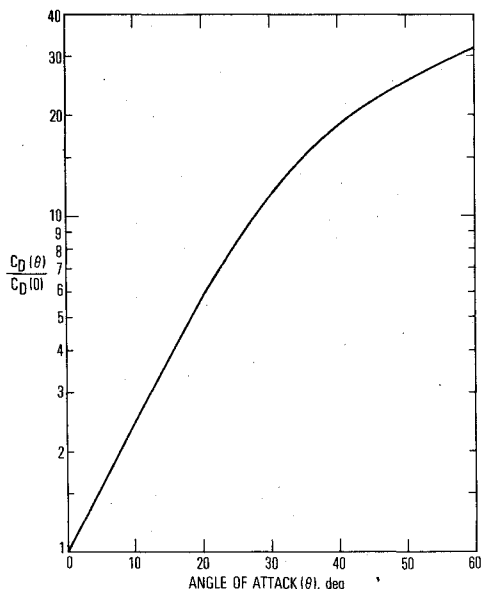


Fig. 2 Drag increase with angle of attack.

limited to 60 deg in the numerical integration. The normal load factor diminishes with decreasing altitude below the altitude at which this 60 deg limit is first reached. It is shown later that very little control moment is required to maintain large angles of attack at the low Mach numbers. Consequently, the vehicle would probably reach its terminal velocity in a flat spin.

The results of Fig. 4 do not include the initial transient required to reach the constant A_N value of angle of attack indicated in the figure. It has been shown¹ that, for small-angle, linear aerodynamics, the angle of attack increases exponentially due to an applied yaw moment M_y according to

$$\begin{aligned} \theta &= \frac{M_y}{2\zeta\omega^2 I} (1 - e^{-\zeta\omega t}) \\ &= \frac{\theta_0^*}{2\zeta} (1 - e^{-\zeta\omega t}) \end{aligned} \quad (5)$$

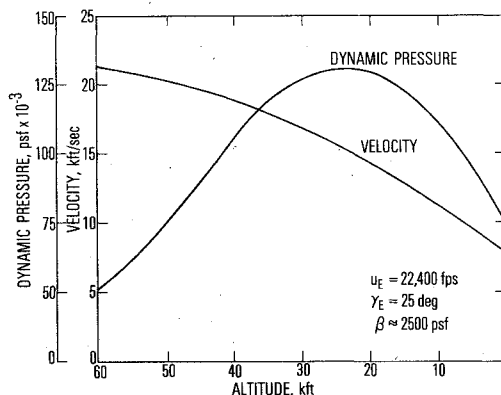


Fig. 3 Reference trajectory.

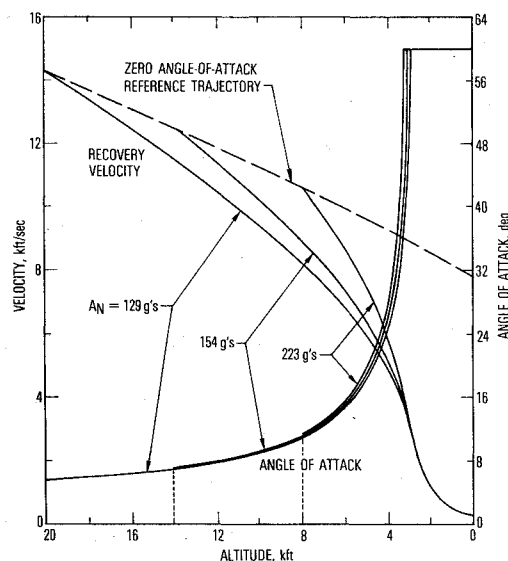


Fig. 4 Recovery velocity and required angle of attack.

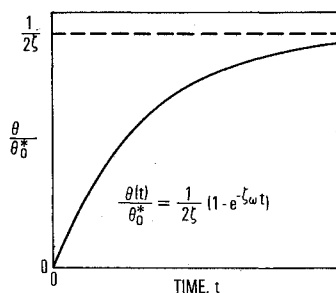


Fig. 5 Yaw-moment undamping of angle of attack.

where $\theta_0^* = M_y / \omega^2 I$ is the nonrolling trim angle of attack that would be produced by the moment M_y if it were body-fixed, and ζ is the aerodynamic pitch or yaw damping expressed as a ratio to critical damping. For a damping ratio ζ in the range of 0.025 to 0.05, this amplifies the trim angle of attack θ_0^* by a factor $2\zeta^{-1}$ of from 10 to 20 after the exponential term $e^{-\zeta\omega t}$ has decayed to a small value. The behavior described by Eq. (5) illustrates the enormous sensitivity of the angle of attack to an applied yaw moment, which is the basis for this control approach. The angle of attack increase expressed by Eq. (5) is shown in Fig. 5. The time required for the angle of attack to increase to 63% of its steady-state value, or $1 - e^{-1}$, is $1/\zeta\omega$. For example, for a natural pitch frequency ω of 100 rad/sec and a damping ratio ζ of 0.04, the time to reach 63% of maximum amplification is 0.25 sec. The vertical descent rate for the 25 deg path angle trajectory is approximately 6 kft/sec, which corresponds to an altitude increment of approximately 1.5 kft for the 0.25 sec transient. The actual transient required to reach the design angle of attack depends on the applied moment which determines the trim angle θ_0^* . At the 20 kft "initiation altitude," the required angle of attack is 5.5 deg. If we assume that this is 63% of the maximum amplified value, i.e., $\theta = 5.5 \text{ deg} = 0.63 \theta_0^* / 2\zeta$, then θ_0^* is 0.70 deg for $\zeta = 0.04$. Therefore, the required yaw moment is that moment that would produce a trim angle of attack of 0.70 deg when applied statically to the nonrolling vehicle. This moment would have to be applied at approximately 21.5 kft in order to achieve the desired angle of attack at 20 kft. The control-force requirements and system implementation are discussed in more detail in the following sections.

III. Control Requirements

The angle-of-attack buildup due to an applied yaw moment has been treated for linear, small-angle aerodynamics.¹ It was shown that the maximum angle of attack is limited by the yaw damping moment in steady coning motion. The aerodynamics of large coning motions can be described in terms of the classical Euler-angle coordinates (Fig. 6) according to^{1,3}

$$\ddot{\theta} + \mu p \dot{\psi} \sin \theta - \dot{\psi}^2 \sin \theta \cos \theta = \frac{M(\theta)}{I} + \frac{M_{\dot{\theta}}}{I} \dot{\theta} \quad (6)$$

$$d/dt(\dot{\psi} \sin \theta) + \dot{\theta} \dot{\psi} \cos \theta - \mu p \dot{\theta} = \frac{M_{\dot{\psi}}}{I} \dot{\psi} \sin \theta + \frac{M_v}{I} \quad (7)$$

$$p = \dot{\phi} + \dot{\psi} \cos \theta \quad (8)$$

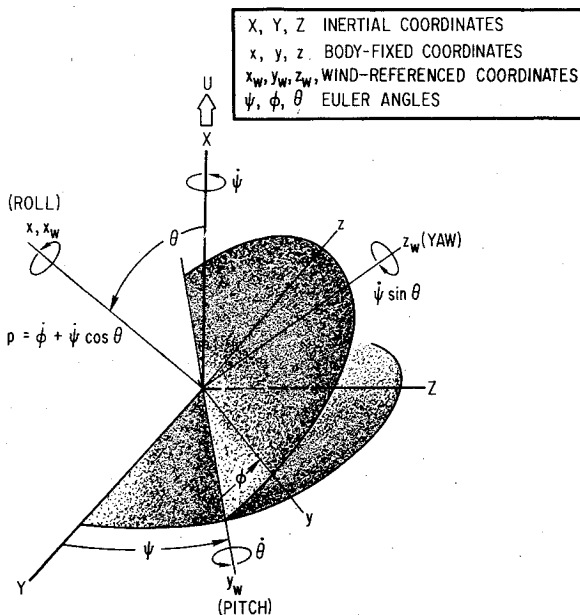


Fig. 6 Euler angle coordinates.

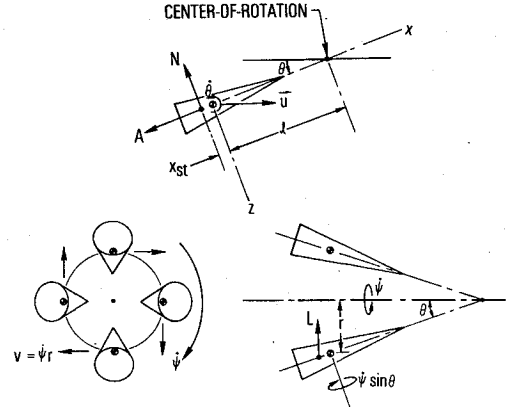


Fig. 7 Coning motion.

where the static pitch moment $M(\theta)$ is

$$M(\theta) = -C_N(\theta) Q S x_{st} \quad (9)$$

M_y is an applied control yaw moment, and $M_{\dot{\theta}}$ and $M_{\dot{\psi}}$ are damping moments per unit rotation rates $\dot{\theta}$ and $\dot{\psi} \sin \theta$. The moment derivatives $M_{\dot{\theta}}$ and $M_{\dot{\psi}}$ consist of both rate damping and normal force damping components caused by translation of the vehicle center of mass. Approximations for these moments can be derived from simple kinematics. For small roll rates such that gyroscopic cross-coupling can be neglected, a statically stable vehicle subjected only to normal and axial forces in the pitch plane θ (Fig. 7a) will rotate about a point a distance $l = I / m x_{st}$ ahead of the center of mass.[†] The effective angle of attack because of rotation $\dot{\theta}$ of the center of mass about this point is $\alpha_{\dot{\theta}} = \dot{\theta} / u = I \dot{\theta} / \mu x_{st}$. This gives rise to a normal force proportional to $C_{N_{\alpha}} \alpha_{\dot{\theta}}$. If we assume a rate damping term proportional to $(C_{m_{\dot{\theta}}} + C_{m_{\dot{\alpha}}}) \dot{\theta}$, we can then write the pitch damping moment derivative

$$M_{\dot{\theta}} = -\frac{C_{N_{\alpha}} Q S I}{\mu u} + (C_{m_{\dot{\theta}}} + C_{m_{\dot{\alpha}}}) \frac{Q S d^2}{2u} \quad (10)$$

The yaw damping moment can be derived in a similar manner. In steady coning motion, the lift force $L(\theta)$ must balance the centrifugal force due to precession $\dot{\psi}$ of the center of mass (Fig. 7b) according to

$$L(\theta) = m \dot{\psi}^2 r \quad (11)$$

The lateral velocity $v = \dot{\psi} r$ gives an effective side-slip angle

$$\beta_{\dot{\psi}} = \dot{\psi} r / u = L(\theta) / \mu u \dot{\psi} \quad (12)$$

which produces normal force damping analogous to that for pitch rate in Eq. (10). If we assume a rate damping term proportional to $(C_{m_{\dot{\psi}}} + C_{m_{\dot{\beta}}}) \dot{\psi} \sin \theta$, where $\dot{\psi} \sin \theta$ is the lateral rate due to precession (yaw rate in the wind-fixed coordinate system), then the yaw damping moment derivative can be written

$$M_{\dot{\psi}} = -\frac{C_{Y_{\beta}} C_L(\theta) Q^2 S^2 x_{st}}{\mu u \dot{\psi}^2 \sin \theta} + (C_{m_{\dot{\psi}}} + C_{m_{\dot{\beta}}}) \frac{Q S d^2}{2u} \quad (13)$$

where $C_{Y_{\beta}}$ is the side force derivative at $\alpha = \theta$, $\beta = 0$. If we consider $C_{Y_{\beta}}(\theta)$ to be the component normal to the θ -plane of the normal force $C_N(\theta_{\text{eff}})$, where θ_{eff} is the induced total angle of attack $(\theta^2 + \beta_{\dot{\psi}}^2)^{1/2}$, then $C_{Y_{\beta}}$ with the definition of $\beta_{\dot{\psi}}$ in Eq. (12) can be written $C_{Y_{\beta}}(\theta) = C_N(\theta) / \sin \theta$. We can approximate $\dot{\psi}$ from Eqs. (6) and (9) for the steady coning condition $\ddot{\theta} = \dot{\theta} = 0$, and small roll rate, which gives

$$\dot{\psi}^2 \sin \theta \cos \theta = C_N(\theta) Q S x_{st} / I \quad (14)$$

[†]The center of rotation is the stationary point where $\ddot{z} = -N/m$ is equal and opposite to $\dot{\theta} = l N x_{st} / I$.

If we substitute this approximation for $\dot{\psi}$ in Eq. (13) with $C_{Y\dot{\theta}} = C_N(\theta)/\sin \theta$, we obtain for the yaw moment damping derivative

$$M_{\dot{\psi}} = -\frac{C_L(\theta) Q S I}{\mu u \tan \theta} + (C_{m_q} + C_{m_{\dot{\alpha}}}) \frac{Q S d^2}{2u} \quad (15)$$

From the yaw equation, Eq. (7), it is shown that, for steady coning $\dot{\theta} = \dot{\psi} = 0$, the applied yaw moment M_y must balance the yaw damping moment

$$M_y = -M_{\dot{\psi}} \dot{\psi} \sin \theta \quad (16)$$

This limiting condition yields a simple approximation for the control moment required to generate a specified coning angle or angle of attack. If we substitute for $\dot{\psi} \sin \theta$ from Eq. (14), the limiting control moment, from Eq. (15), becomes

$$M_y = \frac{C_L(\theta) (QS)^{3/2}}{\mu u} \left[\frac{C_N(\theta) I x_{st}}{\tan \theta} \right]^{1/2} \times \left[1 - \frac{(C_{m_q} + C_{m_{\dot{\alpha}}}) m d^2 \tan \theta}{2 I C_L(\theta)} \right] \quad (17)$$

If we make the further approximations $C_L(\theta) \approx C_N(\theta) \cos \theta$, $C_{N\dot{\alpha}} \approx C_N(\theta)/\sin \theta$, and substitute $A_N = C_N(\theta) Q S / m g$, Eq. (17) reduces to

$$M_y = A_N g \cos^{3/2} \theta \left[\frac{C_{N\dot{\alpha}} \rho S I x_{st}}{2} \right]^{1/2} \times \left[1 - \frac{(C_{m_q} + C_{m_{\dot{\alpha}}}) m d^2}{2 I C_{N\dot{\alpha}} \cos^2 \theta} \right] \quad (18)$$

The moment given by Eq. (17) or (18) is the applied yaw moment required to sustain steady coning motion at the coning half-angle θ . This moment does not account for the time delay to reach the steady-state value, described qualitatively by Eq. (5) and Fig. 5, and, therefore, represents a lower limit on the required control moment. Equation (18) is independent of velocity and indicates that, for constant A_N recovery, the required control moment remains reasonably constant until the coning angle θ becomes moderately large.† This is illustrated in Fig. 8 which shows the control force $F_y = M_y/x_c$, calculated from Eq. (17), required to generate the angle-of-attack and velocity histories of Fig. 4 with different altitudes of recovery initiation. The vehicle and aerodynamic parameters used in the calculation are

$mg = 200 \text{ lb}$	$I = 5.13 \text{ slug-ft}^2$
$L = 4 \text{ ft}$	$I_N = 0.385 \text{ slug-ft}^2$
$d = 1.20 \text{ ft}$	$C_{N\dot{\alpha}} = 1.9$
$S = 1.14 \text{ ft}^2$	$C_{m_q} + C_{m_{\dot{\alpha}}} = -2.5$
$x_c = 1.68 \text{ ft}$	$p = 1.5 \text{ rps}$
$x_{st} = 5\% L$	

The two terms in the second bracket of Eqs. (17) and (18) represent the relative contributions of normal force and rate damping, normalized with respect to the normal force component. The effective sideslip angle $\beta_{\dot{\psi}}$ in Eq. (12), which determines the normal force damping component, is quite small even for large values of θ . Therefore, the linear, small-angle normal force derivative should give a reasonable approximation to this moment for conditions of practical interest. However, the rate damping term was assumed to be proportional to the linear damping-in-pitch derivative $C_{m_q} + C_{m_{\dot{\alpha}}}$, which is only valid for small-to-moderate values of the coning half-angle. Experimental studies of this moment for large circular coning motions of a sharp 10 deg half-angle cone at supersonic Mach numbers^{4,6} indicate that the linear damping-in-pitch approximation is valid for coning half-angles up to approximately 1.5 times the cone half-angle. For larger coning angles, the yaw-rate damping moment becomes

†The decrease in M_y with increasing θ through the $\cos \theta$ term is somewhat compensated for by the density increase with decreasing altitude.

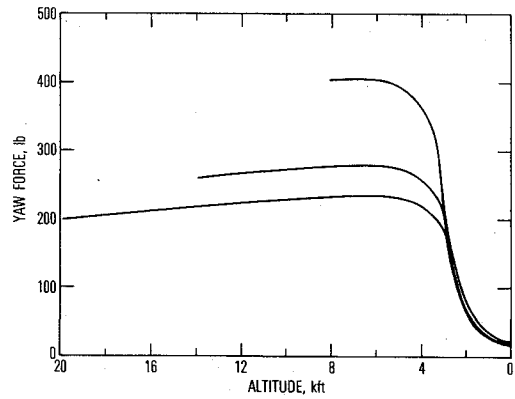


Fig. 8 Required control force.

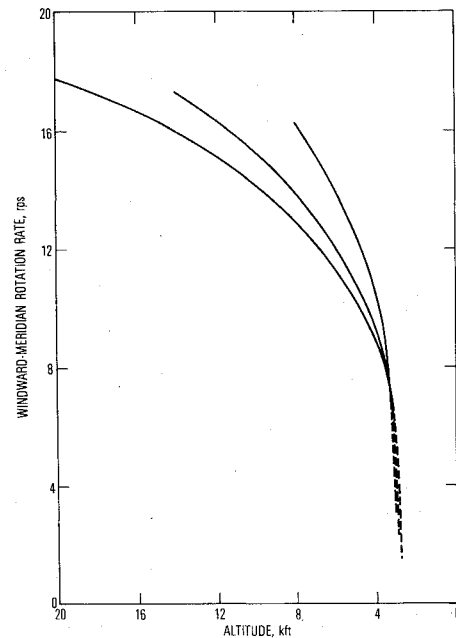


Fig. 9 Windward-meridian rotation rate.

nonlinear, reaches a peak value, and tends toward destabilizing values with increased coning angle. The peak value occurs at approximately twice the cone half-angle.

A constant value of -2.5 for $C_{m_q} + C_{m_{\dot{\alpha}}}$ was used in the force calculation of Fig. 8, based on experimental data for a sharp, 9 deg cone at Mach. 10.⁷ The yaw damping moment (required control force) diminishes rapidly as the angle of attack exceeds approximately twice the cone half-angle, the point at which $C_{m_q} + C_{m_{\dot{\alpha}}}$ tends toward destabilizing values based on the earlier observations.^{4,6} Consequently, a precise determination of $C_{m_q} + C_{m_{\dot{\alpha}}}$ at the larger angles of attack does not appear to be a stringent requirement for predicting the required control moment, at least for the relative magnitudes of normal force and rate damping representative of the preceding example. For configurations such that the rate damping term predominates, i.e., the second term in the right-most bracket of Eqs. (17) and (18) is much larger than unity, the coefficient $C_{m_q} + C_{m_{\dot{\alpha}}}$ would have a strong influence on the total damping moment and the required control force. The rapid decrease of damping moment with increased angle of attack is the basis for the earlier statement that the vehicle would probably reach terminal velocity in a flat spin, i.e., near 90 deg angle of attack. Such behavior has been observed during Magnus-type instabilities of spinning missiles.⁸

A characteristic of yaw-moment undamping of angle of attack is a rapid rotation of the vehicle relative to the wind (windward-meridian rotation rate). This has a beneficial effect of distributing the heat load uniformly around the vehicle, but also requires that a control force generated from a body-fixed thruster or trim generator be modulated at the

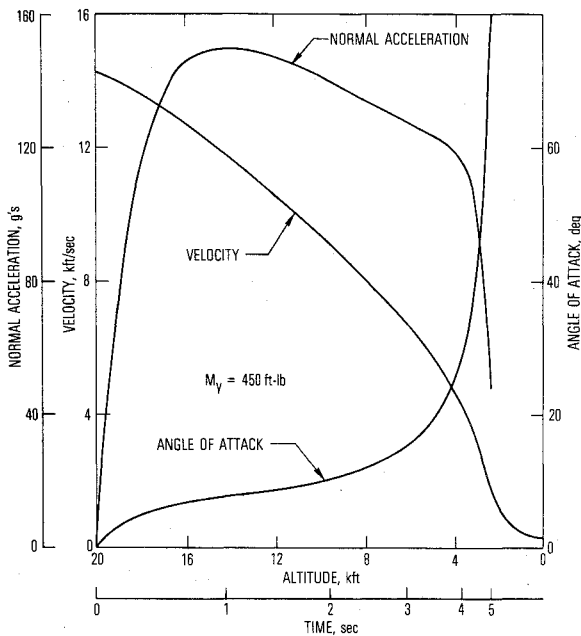


Fig. 10 Response to constant control moment applied at 20 kft.

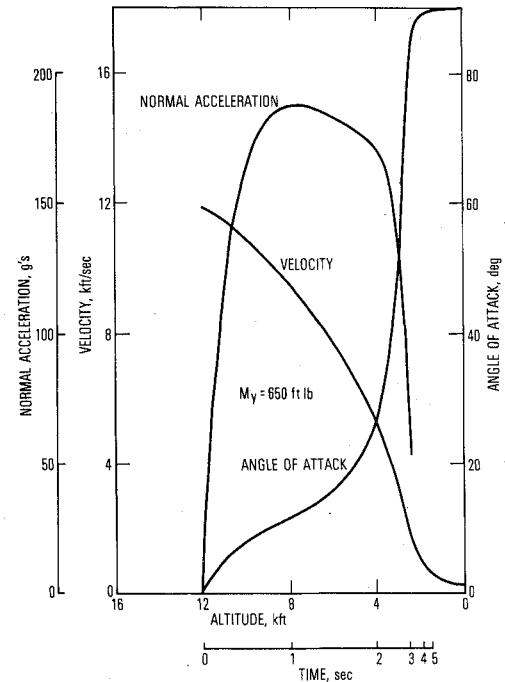


Fig. 12 Response to constant control moment applied at 12 kft.

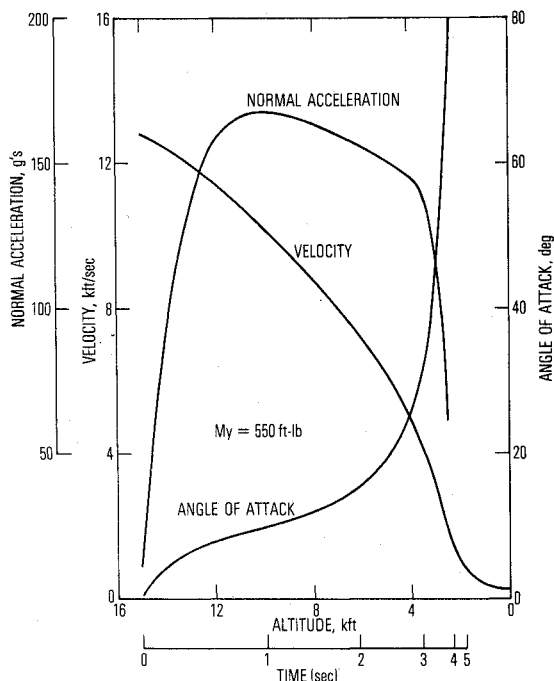


Fig. 11 Response to constant control moment applied at 15 kft.

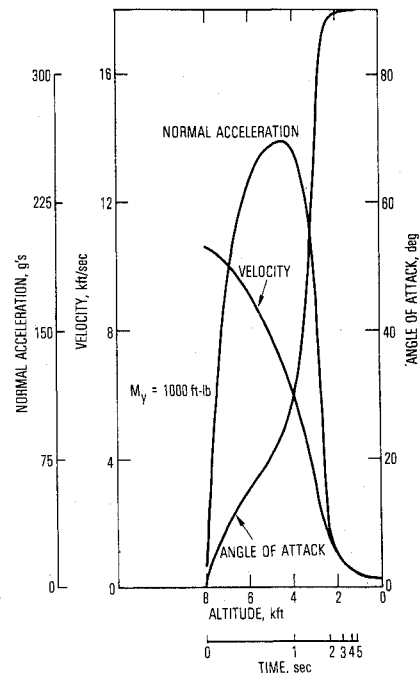


Fig. 13 Response to constant control moment applied at 8 kft.

windward-meridian rotation frequency in order to produce a net yaw force. The windward-meridian rotation rate, from Eq. (8), has one of the characteristic frequencies

$$\dot{\phi}_{+,-} = p - \dot{\psi}_{+,-} \cos \theta \quad (19)$$

where $\dot{\psi}_{+,-}$ are approximately the positive and negative roots of Eq. (14). A more precise definition of $\dot{\psi}_{+,-}$, from Eq. (6) with $\theta = \dot{\theta} = 0$, yields

$$\dot{\psi}_{+,-} = (p_r / \cos \theta) \pm \left[(p_r / \cos \theta)^2 + \frac{C_N(\theta) Q S x_{SV}}{I \sin \theta \cos \theta} \right]^{1/2} \quad (20)$$

where $p_r = \mu p / 2$, and the prevalent mode of $\dot{\psi}_{+,-}$ and $\dot{\phi}_{+,-}$ depends on the direction of the applied yaw moment. The windward-meridian rotation rate that corresponds to the positive precession mode of Eq. (20) is shown in Fig. 9 for the recovery conditions of Fig. 4 and a roll rate p of 1.5 rps.

It is somewhat fortuitous that the control moment required for constant A_N recovery is reasonably constant over a large portion of the trajectory. This would facilitate the design of a recovery system in which reaction jets, for example, are used to generate the control moment. The vehicle response to a constant control moment is shown in Figs. 10-13, which are obtained from a numerical integration of the coupled vehicle and trajectory equations of motion, Eqs. (1-3) and (6-8). Figures 10-13 correspond to constant control forces of 267, 325, 387, and 593 lb applied at 20, 15, 12, and 8 kft, respectively, such to decelerate the vehicle to Mach 1 by 2 kft. The angle of attack is not constrained as in Fig. 4 and rapidly approaches 90 deg. Peak values of normal acceleration are 150, 167, 188, and 262 g's for the 20, 15, 12, and 8 kft initiation altitudes, respectively. The initial angle-of-attack transients

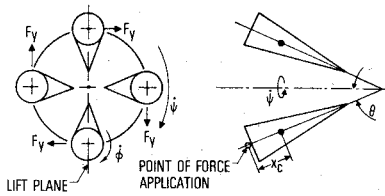


Fig. 14 Control implementation.

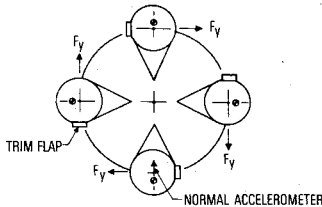


Fig. 15 Roll resonance recovery concept.

are well-described by the linear theory of Eq. (5). For the 20 kft initiation (Fig. 10), the applied yaw moment corresponds to an equivalent trim angle of attack θ_0^* of approximately 0.5 deg. The initial pitch frequency ω is approximately 100 rad/sec, and the damping ratio ζ is 0.033 which results in an exponential buildup of angle of attack to approximately 6 deg in 0.5 sec. For the 15-kft initiation, θ_0^* is approximately 0.6 deg, and similar values for ω and ζ as for 20 kft yield a predicted angle of attack of approximately 7.5 deg in 0.5 sec. The large excursion in angle of attack at lower altitude is a consequence of the decrease in yaw damping moment with increased angle of attack, discussed in conjunction with Fig. 8. These results were obtained with a constant value of $C_{mq} + C_{m\dot{\alpha}}$ and do not take into account the observed decrease in this parameter with increased coning angle.^{4,6} This would cause even a further decrease in the damping moment and a more rapid angle of attack response to a constant applied yaw moment at the larger angles of attack.

IV. System Implementation

Implementation of the control system requires a means of generating a wind-fixed yaw moment, i.e., a control force that acts perpendicular to the lift plane at some axial distance from the vehicle center-of-mass, as shown in Fig. 14. Since the vehicle rotates relative to the lift plane at the rate $\dot{\phi}$, a control force generated from a body-fixed thruster or control surface must be modulated at the frequency $\dot{\phi}$, typical values of which are shown in Fig. 9. An exception to this occurs during steady roll resonance when $p = \psi + \cos \theta$, and $\dot{\phi}$ defined by Eq. (19) is zero. For this case, a body-fixed trim force becomes a yaw force,¹ and the trim angle of attack is amplified according to Eq. (5). A simple recovery system based on resonance is discussed later. For the nonresonance case, the yaw force can be generated with one or more body-fixed reaction jets or trim flaps servoed in a simple control loop with a normal accelerometer in order to sense the lift orientation and windward-meridian rotation rate. The thruster or trim flap is modulated to provide a net yaw force with each revolution of the vehicle relative to the wind. Alternatively, a pendulum mass might be used to take advantage of the large normal accelerations and thereby orient a thruster or trim generator relative to the lift plane. The pendulum (and thruster) would rotate with the lift vector relative to the vehicle at the windward-meridian rotation frequency. Several schemes have been described¹ for generating a yaw moment by using this principle. Such systems should be easy to implement with the stabilizing effect of the large normal accelerations during recovery, but have the disadvantage of requiring a mechanical decoupling of the force generator from the vehicle.

The results of Figs. 10-13 indicate that a control force of the order of 250 to 600 lb could be required to recover a 200 lb vehicle flying the reference trajectory, depending on the altitude of recovery initiation. The total impulse required is of the order of 1000 lb sec. We can extrapolate these results to

different size vehicles by using the parametric dependence of control moment described by Eqs. (17) or (18). If we assume that the vehicle mass varies as the base area, in order to maintain a constant ballistic coefficients, we find that the required control force for a geometrically similar configuration varies as the 1.25 power of vehicle weight. For example, the required control force and total impulse for a 115 lb vehicle would be one-half of the above values calculated for the 200 lb vehicle. On the basis of these results, it would appear that reaction jets could be used to generate the control moment for recovery of re-entry vehicles in the 100 to 200 lb weight class. For larger vehicles or higher-energy trajectories, or both, the force and impulse requirements could reach levels that are impractical to achieve with reaction jets. The alternative to reaction jets is aerodynamic control surfaces such as small trim flaps. The required force levels are quite minimal at re-entry hypersonic Mach numbers. This is indicated by the small equivalent trim angle of attack θ_0^* that would be produced by the control moment M_y if it were body-fixed (Eq. 5). The control moments required for recovery in the examples of Figs. 10-13 correspond to equivalent trim angles of attack at recovery initiation of the order of 0.5 to 1 deg. Although the yaw moment must be modulated at the windward-meridian rotation frequency (Fig. 9), this should not be difficult to implement at these relatively small force levels.

An alternative control scheme eliminates the requirement for modulating the control force and provides possibly the simplest concept for an effective re-entry vehicle recovery system. The concept consists of a controllable aerodynamic trim flap in conjunction with a center-of-gravity offset normal to the trim plane (Fig. 15). The combined mass and aerodynamic asymmetry will spin the vehicle rapidly into steady roll resonance.^{3,9} In this condition, the vehicle is in lunar motion ($\dot{\phi} = 0$), and the trim force rotates 90 deg out of the lift plane to become a steady yaw force. The trim is controlled by means of a normal accelerometer aligned in the center-of-gravity offset plane to maintain a specified normal g-factor. As an alternative to the trim flap, the system could use reaction jets in the plane of a fixed aerodynamic trim. The thrusters would augment the fixed aerodynamic trim to sustain the required normal acceleration level. Unlike the nonresonance system, the resonance concept results in lunar motion and, consequently, subjects the vehicle to sustained heating on the windward ray at angles of attack. This might be desirable in some instances for studying the influence of angle of attack on ablation.

V. Conclusions

The drag increase of a high-ballistic-coefficient re-entry vehicle with angle of attack is sufficient for recovery at altitudes below 20 kft. Yaw-moment undamping provides an effective means of inducing large circular coning motion with little expenditure of energy. Required yaw moments are sufficiently small that reaction jets can probably be used for vehicles up to 200 lb flying high-energy trajectories. Yaw-moment undamping also causes a rapid rotation of the vehicle relative to the wind; this dissipates the recovery energy uniformly in heating over the entire vehicle. Roll resonance-induced coning motion from combined mass and aerodynamic asymmetries provides a simple alternative recovery concept based on angle-of-attack control of drag.

References

- Platus, D.H., "Angle-of-Attack Control of Spinning Missiles," *Journal of Spacecraft and Rockets*, Vol. 12, April 1975, pp. 228-234.
- Foster, A.D., "A Compilation of Longitudinal Aerodynamic Characteristics Including Pressure Information for Sharp and Blunt Nose Cones Having Flat and Modified Bases," Sandia Corp., Albuquerque, N. M., SC-R-64-1311, Jan. 1965.
- Platus, D.H., "A Simple Analysis of Re-entry Vehicle Roll Resonance," Air Force Space Systems Division, SSD-TR-67-25, El Segundo, Calif., Jan. 1967.

⁴Tobak, M., Schiff, L.B., and Peterson, V.L., "Aerodynamics of Bodies of Revolution in Coning Motion," *AIAA Journal*, Vol. 7, Jan. 1969, pp. 95-99.

⁵Schiff, L.B. and Tobak, M., "Results from a New Wind-Tunnel Apparatus for Studying Coning and Spinning Motions of Bodies of Revolution," *AIAA Journal*, Vol. 8, Nov. 1970, pp. 1953-1957.

⁶Schiff, L.B., "Nonlinear Aerodynamics of Bodies in Coning Motion," *AIAA Journal*, Vol. 10, Nov. 1972, pp. 1517-1522.

⁷Ward, L.K., Jr. and Mansfield, A.C., "Dynamic Characteristics of a 9 deg Cone with and without Asymmetries at Mach 10," Arnold Engineering Development Center, Tenn., AEDC-TR-70-1, March 1970.

⁸Nicolaides, J.D., "Two Non-Linear Problems in the Flight Dynamics of Modern Ballistic Missiles," Institute of the Aeronautical Sciences, N. Y., IAS No. 59-17, Jan. 1959.

⁹Pettus, J.J., "Persistent Re-Entry Vehicle Roll Resonance," AIAA Paper 66-49, New York City, N. Y., Jan. 1966.

From the AIAA Progress in Astronautics and Aeronautics Series . . .

FUNDAMENTALS OF SPACECRAFT THERMAL DESIGN—v. 29

Edited by John W. Lucas, Jet Propulsion Laboratory

The thirty-two papers in this volume review the development of thermophysics and its constituent disciplines in relation to the space program, together with concerns for future development, in fields of surface radiation properties, thermal analysis, heat pipes, and thermal design.

Surface radiation covers ultraviolet and particle radiation of pigments, paints, and other surfaces, both coated and uncoated, in thermal control applications. Optical characteristics of variously degraded and exposed surfaces are also considered. Thermal analysis studies consider radiative heat transfer, thermal resistance, reentry thermal analysis, and modeling for spacecraft thermal analysis.

Heat pipes section covers friction, electro-osmosis, grooved pipes, organic-fluid pipes, gas-controlled pipes, variable-conductance pipes, and specific heat pipe designs and applications.

Thermal design topics include the Apollo telescope mount, the space shuttle orbiter wing cooling system, and methods and selection criteria for thermal control of a twelve-person space station.

599 pp., 6 x 9, illus. \$14.00 Mem. \$20.00 List

TO ORDER WRITE: Publications Dept., AIAA, 1290 Avenue of the Americas, New York, N. Y. 10019